Insights into Nucleotide Signal Transduction in Nitrogenase: Structure of an Iron Protein with MgADP Bound[†,‡]

Se Bok Jang, Lance C. Seefeldt,* and John W. Peters*

Department of Chemistry and Biochemistry, Utah State University, Logan, Utah 84322

Received July 24, 2000; Revised Manuscript Received September 18, 2000

ABSTRACT: Coupling the energy of nucleoside triphosphate binding and hydrolysis to conformational changes is a common mechanism for a number of proteins with disparate cellular functions, including those involved in DNA replication, protein synthesis, and cell differentiation. Unique to this class of proteins is the dimeric Fe protein component of nitrogenase in which the binding and hydrolysis of MgATP controls intermolecular electron transfer and reduction of nitrogen to ammonia. In the work presented here, the MgADP-bound (or "off") conformational state of the nitrogenase Fe protein has been captured and a 2.15 Å resolution X-ray crystal structure is presented. The structure described herein reveals likely mechanisms for long-range communication from the nucleotide-binding sites for controlling the affinity of association with the MoFe protein component. Two pathways, termed switches I and II, appear to be integral to this nucleotide signal transduction mechanism. In addition, the structure provides the basis for the changes in the biophysical properties of the [4Fe-4S] cluster observed when Fe protein binds nucleotides. The structure of the MgADP-bound Fe protein provides important insights into the respective contributions of nucleotide interaction and complex formation in defining the conformational states that are the keys to nitrogenase catalysis.

Numerous proteins, with cellular functions ranging from cell division to molecular motion, couple the energy from the binding or hydrolysis of nucleoside triphosphates (e.g., ATP or GTP) to drive protein conformational changes (*1*−*5*). These protein conformational changes are often propagated over some distance (>10 Å) to activate a downstream function in the cell or to define an "on" or "off" state of the protein. The bacterial enzyme nitrogenase is a unique member of this class of nucleotide-utilizing enzymes coupling the energy of nucleotide binding and hydrolysis to electron-transfer reactions within a macromolecular complex (*7*). Nitrogenase catalyzes the reduction of N_2 to NH_3 in a reaction that is usually depicted as shown in eq 1.

$$N_2 + 8H^+ + 16MgATP + 8e^- \rightarrow 2NH_3 + H_2 + 16MgADP + 16P_i \quad (1)$$

In this case, MgATP binding and hydrolysis control several different aspects of the mechanism. Nitrogenase is composed of two component proteins called the Fe protein and the MoFe protein. Nucleotides bind to the homodimeric Fe protein, which also contains a single [4Fe-4S] cluster. One function of MgATP binding and hydrolysis is to regulate the transfer of an electron from the [4Fe-4S] cluster to the MoFe protein. The ultimate acceptor of electrons in the MoFe protein is a mixed metal cluster called the FeMo cofactor, where substrates bind and are reduced (*9*). Following each electron-transfer event, the Fe protein dissociates from the MoFe protein (*10*), and the oxidized Fe protein is reduced concomitant with the replacement of the MgADP molecules with MgATP. The hydrolysis of MgATP to MgADP appears to regulate the affinity for association between the Fe protein and the MoFe protein. This is essential to the reaction since all substrate reduction reactions catalyzed by nitrogenase require two or more electrons.

As is common among the general class of nucleotide-utilizing proteins, MgATP acts at a distance to accomplish these changes in the nitrogenase mechanism (*8*). Nucleotides bind to the Fe protein more than 15 Å away from the clusters involved in electron transfer and the protein surfaces involved in Fe protein−MoFe protein docking. This architecture for the Fe protein demands that the energy of nucleotide binding and hydrolysis be manifested as protein conformational changes that are communicated to the [4Fe-4S] cluster and to the protein−protein docking surface. A working model is that a continuum of protein conformational changes is dictated by the binding of MgATP, the hydrolysis of P_i, the loss of P_i, the repositioning of Mg^{2+} ion, and finishing with the MgADP-bound or off state. In an effort to understand the nature of the nucleotide-induced protein conformational changes and how these impact the nitrogenase mechanism, we have captured the Fe protein in a MgADP-bound state and determined the X-ray crystal structure by X-ray diffraction methods. This structure, in conjunction with an earlier structure of the Fe protein−MoFe protein complex trapped with ADP AlF_4^- (*11*), provides insights into how specific regions of the Fe protein might act to transduce nucleotide interactions to changes in metal clusters and the association between the nitrogenase component proteins.

[†] This research was supported by USDA Grant 98-353-05-6552 to J.W.P. and NSF Grant MCB-9722937 to L.C.S.

[‡] Atomic coordinates for this structure have been deposited in the RCSB Protein Data Bank for release upon publication (entry 1FP6).

* To whom correspondence should be addressed. J.W.P.: e-mail, petersj@cc.usu.edu.

10.1021/bi001705g CCC: $19.00
Published on Web 11/08/2000

Table 1: Data and Refinement Statistics

Cell Parameters	
space group	$P2_12_12_1$
cell dimensions	$a = 93.25$ Å
	$b = 119.53$ Å
	$c = 120.94$ Å
Data Statistics	
resolution (Å)	30.0−2.15
completeness (%) (last cell)	88.8 (69.4)
no. of observed reflections	210392
no. of unigue reflections	65315
I/σ	7.7 (2.6)
R_{merge} (%)[a] (highest-resolution bin)	6.4 (27.9)
Crystallographic Refinement	
no. of protein non-hydrogen atoms	8816
no. of MgADP molecules	4.0
MgADP occupancy	1.0
R_{cryst}[b]	0.200
R_{free}[c]	0.267
deviations from ideal geometry	
bond lengths (Å)	0.009
bond angles (deg)	2.362
Ramachandran Statistics (% of total residues)	
most favored regions	90.9
additional allowed regions	9.1
generously allowed regions	0.0
disallowed regions	0.0

[a] $R_{merge} = \Sigma_{hkl}\Sigma_i|I_i - \langle I\rangle/\Sigma_{hkl}\Sigma_i|\langle I\rangle|$, where I_i is the intensity for the ith measurement of an equivalent reflection with indices h, k, and l. [b] $R_{cryst} = \Sigma_{hkl}||F_{obs}| - |F_{calc}||/\Sigma_{hkl}|F_{obs}|$, where F_{obs} denotes the observed structure factor amplitude and F_{calc} denotes the structure factor amplitude calculated from the model. [c] Five percent of the reflections were used to calculate R_{free}.

MATERIALS AND METHODS

Expression and purification of the Fe protein were accomplished as previously described (*12*). The Fe protein was purified in 50 mM Tris buffer (pH 8.0) in the presence of 2 mM sodium dithionite and included 20% glycerol as a stabilizing agent. Protein was protected from oxygen by manipulation in sealed serum vials with 2 mM dithionite or in an argon atmosphere glovebox (Vacuum Atmospheres, Hawthorne, CA).

The Fe protein was crystallized by microcapillary batch diffusion (*8*) using 30% PEG 4000, 0.1 M Tris-HCl (pH 8.5), 0.2 M sodium acetate, and 18% glycerol as precipitating solutions. The Fe protein crystals are brown in color and grow in ~7 days to an average size of 0.3 mm × 0.4 mm × 0.6 mm. Prior to crystallization, MgADP was added to the protein to a final concentration of 10 mM. The crystals were flash-cooled in liquid nitrogen on rayon loops, and data were collected under a continuous nitrogen stream at approximately 100 K. X-ray diffraction data were collected at Stanford Synchrotron Radiation Laboratory Beamline 9-1 ($\lambda = 0.97$ Å) using ϕ scans with a scan width of 1.0°. The data were processed using MOSFLM (*13*) and scaled using SCALA of the CCP4 suite of computer programs (*14*). The crystals belong to orthorhombic space group $P2_12_12_1$ ($a = 93.25$ Å, $b = 119.53$ Å, and $c = 120.94$ Å) containing two Fe protein dimers and four MgADP molecules in the asymmetric unit (~120 kDa). A total of 210 392 reflections were measured which were reduced to 65 315 unique reflections representing 88.8% of a complete 2.15 Å data set.

The structure was determined by the molecular replacement method by AMORE (*15*) using the Fe protein model 1nip as a search model. The search was carried out with the data between 12.0 and 5.0 Å; the first molecule had a correlation coefficient of 33.0 ($R = 51.4\%$), and the solution of the second molecule resulted in a correlation coefficient of 46.8 ($R = 46.3\%$). The model was improved through iterative model building using the program O (*16*). During refinement, a bulk solvent correction allowed the inclusion of all low-resolution reflections and ~5% of the data were randomly selected for cross validation (*17*). Model bias was removed for the incorporation of R_{free} calculation for cross validation by randomization using the simulated annealing routine of X-PLOR (*18*) with an annealing temperature of 4000 K. The noncrystallographic symmetry was exploited during refinement by restraining chemically identical chains of the individual Fe protein dimers to an overall rms deviation of corresponding Cα atoms of 0.032 Å. Initial positional refinement of the rigid-body-refined model using 30.0−2.15 Å data followed by group *B*-factor refinement dropped the R_{free} to 44.0%. In the final stages of refinement, the quality of the model was improved by gradually releasing the NCS restraints. The final model has been refined to 2.15 Å resolution to a current R_{cryst} of 20.0% and an R_{free} of 26.7% and consists of all 1148 possible protein residues, two [4Fe-4S] clusters, four MgADP molecules, and 1294 water molecules (Table 1). The model obeys good geometry, with rms deviations from ideal bond lengths and angles of 0.009 Å and 2.388°, respectively, and has 100% of its amino acid residues in allowed regions of a Ramachandran plot (*19*).

Table 2: Side Chain and Main Chain Interactions at the MgADP Site[a]

	WT MgADP (Å)	AlF (Å)
base		
Asn185($O_{\delta1}$)−ADP(N_6)	4.17 ± 0.09	3.52 ± 0.01
Asn185($O_{\delta1}$)−ADP(N_7)	3.12 ± 0.18	3.40 ± 0.01
Pro212(O)−ADP(N_6)	3.03 ± 0.18	3.27 ± 0.01
Pro212(O)−ADP(N_1)	3.97 ± 0.04	4.43 ± 0.01
Asp214(O)−ADP(N_1)	3.53 ± 0.07	3.33 ± 0.06
Asp214(N)−ADP(N_1)	3.27 ± 0.15	3.26 ± 0.01
Arg213($N_{\gamma1}$)−ADP(N_3)	6.57 ± 0.13	3.03 ± 0.01
Gln218($O_{\epsilon1}$)−ADP(N_3)	3.06 ± 0.12	3.40 ± 0.01
Gln236($N_{\epsilon1}$)−ADP(N_6)	3.43 ± 0.16	3.79 ± 0.01
Tyr240(O_η)−ADP(N_6)	3.70 ± 0.17	4.25 ± 0.01
sugar		
Glu221($O_{\epsilon2}$)−ADP($O_{2'}$)	2.80 ± 0.06	2.97 ± 0.01
phosphate		
Lys10(O)−ADP(O_7)	3.64 ± 0.04	3.94 ± 0.01
Gly12(N)−ADP(O_7)	3.46 ± 0.10	2.93 ± 0.01
Ile13(N)−ADP(O_7)	3.35 ± 0.09	3.00 ± 0.01
Gly14(N)−ADP(O_6)	3.21 ± 0.04	3.18
Lys15(N_ζ)−ADP(O_{22})	2.82 ± 0.20	2.78 ± 0.01
Lys15(N)−ADP(O_7)	3.03 ± 0.06	2.60 ± 0.01
Ser16(N)−ADP(O_{22})	3.07 ± 0.10	2.61 ± 0.02
Ser16(O_γ)−ADP(O_{22})	3.20 ± 0.04	3.01 ± 0.02
Thr17(N)−ADP(O_{11})	2.90 ± 0.10	2.74
Thr17($O_{\gamma1}$)−ADP(O_{11})	3.22 ± 0.20	2.99 ± 0.0
Mg^{2+}		
Ser16(O_γ)−Mg^{2+}	2.28 ± 0.03	2.37 ± 0.01
Asp43($O_{\delta2}$)−Mg^{2+}	3.77 ± 0.05	3.71 ± 0.01
Asp39($O_{\delta2}$)−Mg^{2+}	3.90 ± 0.17	2.94 ± 0.02
ADP(O_{22})−Mg^{2+}	2.23 ± 0.04	3.56 ± 0.02
Asp125($O_{\delta2}$)−Mg^{2+}	4.49 ± 0.27	3.79 ± 0.01

[a] The given distances represent an average from the four MgADP binding sites of each structure. Individual errors associated with a given distance indicate the deviation of the distances in the four nucleotide binding sites in the structures [the two Fe protein molecules in the nitrogenase complex (AlF) (*11*) and the two Fe protein dimers in the asymmetric unit of the MgADP-bound Fe protein (WT MgADP)].

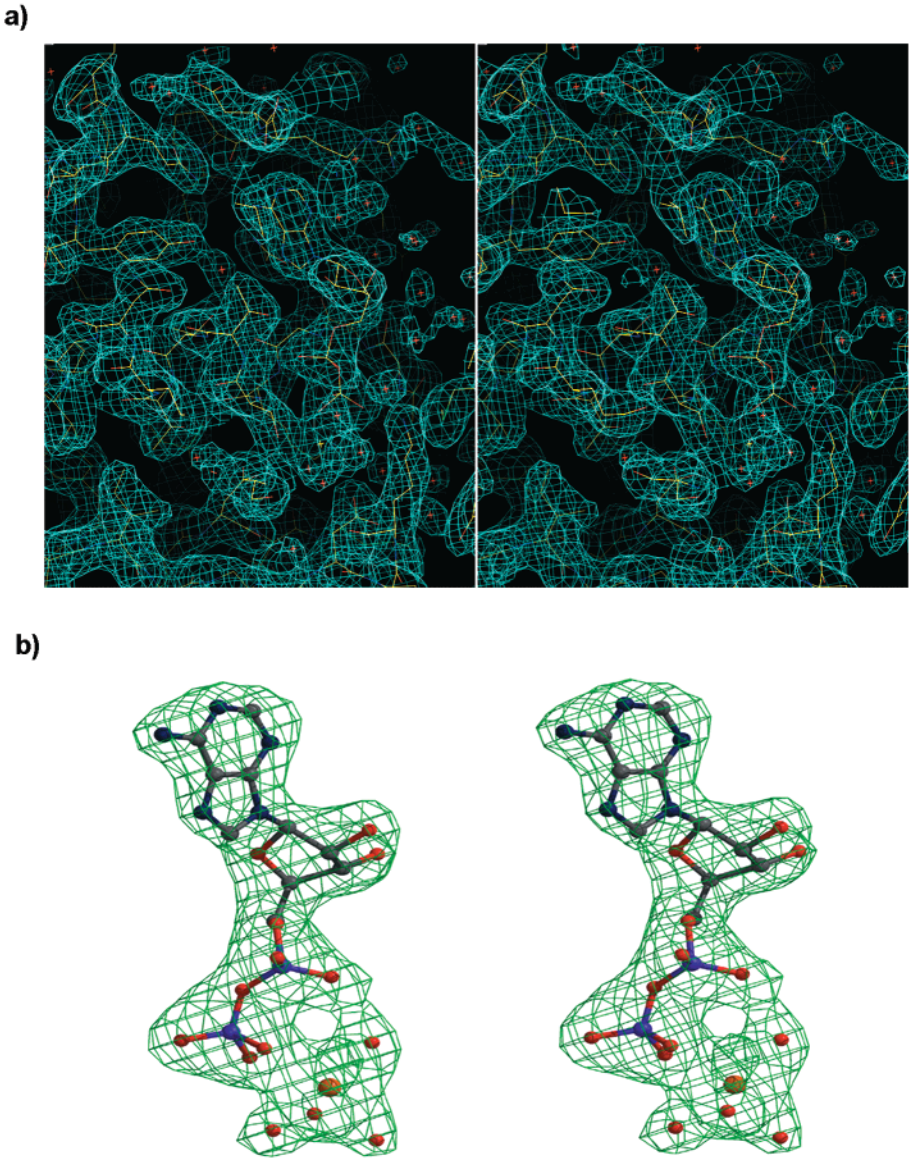

FIGURE 1: (a) Electron density maps ($2F_o - F_c$) contoured at 1σ of a molecule of bound MgADP and its associated polypeptide within a single monomer of the Fe protein dimer. (b) Difference electron density maps ($F_o - F_c$) contoured at 3.5σ in which the MgADP and associated water molecules are omitted from the structure factor and phase calculation.

The structural representations in Figures 1−5 were generated in O (*16*), BOBSCRIPT (*20*), RASTER3D (*21*), and GRASP (*22*).

RESULTS AND DISCUSSION

The structure of the nitrogenase Fe protein in the presence of MgADP has been determined at 2.15 Å resolution. The result of refinement and the quality of electron density maps (Figure 1a,b) indicate that the MgADP is present at full occupancy, allowing the full extent of MgADP-dependent conformational changes to be observed. The two MgADP molecules bound to the Fe protein are located near the dimer interface, one on each subunit (Figure 2a,b). The nucleotide molecules are oriented parallel to the 2-fold symmetry axis with the β-phosphates pointing in the direction of the [4Fe-4S] cluster. This binding orientation is consistent with the orientation of GDP binding to ras P21 (*5*), and contrasts with an across subunit binding mode reported previously for low-occupancy ADP bound to the Fe protein (*8*). Entry of the MgADP molecules into the two binding sites on the Fe protein appears to be from the face opposite the [4Fe-4S] cluster (Figure 2c). Channels leading to the MgADP binding sites terminate in a region with significant negative charge. The majority of the negative charges come from three aspartate residues (Asp39, Asp43, and Asp125) that participate in the coordination of the Mg^{2+} ion either directly or through bound water molecules. The extent of the channel is clearly large enough for MgADP molecules to freely access the site in the MgADP-bound state of the protein (Figure 2c, left panel). This contrasts with a decrease in the level of access observed in the nitrogenase complex stabilized in the presence of MgADP and tetrafluoroaluminate (*11*) (Figure 2c, right panel). The closure of the channel in the Fe protein−MoFe protein complex results from a dramatic rigid-body reorientation of the Fe protein subunits with respect to one another, bringing the subunit interface of the Fe protein monomers closer together.

A number of amino acids within the Fe protein are observed to reposition in order to accommodate the binding

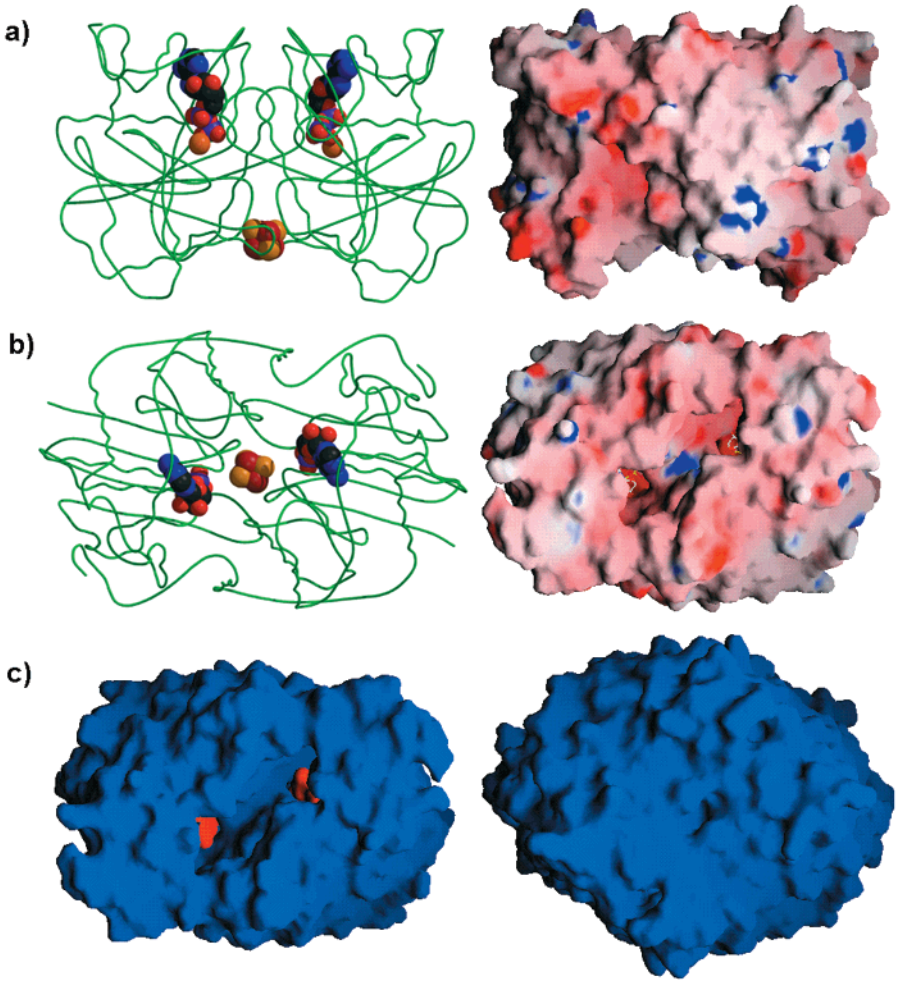

FIGURE 2: Structure of nitrogenase Fe protein with MgADP or MgADP AlF_4^- bound. (a) Coil representation of the Fe protein with MgADP bound with the [4Fe-4S] cluster and MoFe protein interface at the bottom and two MgADP molecules near the top in space-filling representations. The left figure shows a Cα trace, and the right figure shows a space-filling model relative distribution of surface charge shown with acidic regions in red, basic regions in blue, and neutral regions in white. (b) Same representation as in panel a except the view is of the [4Fe-4S] distal face of the Fe protein showing the region of the protein which permits access to the nucleotide binding site. MgADP molecules are shown as stick models. (c) Surface representation of the Fe protein with MgADP bound (left) or MgADP AlF_4^- (right) viewed from the top (same as panel b) with MgADP molecules shown in red. These figures were generated using the programs BOBSCRIPT (*20*) and GRASP (*22*).

of MgADP. The adenine base is bound to the Fe protein through interactions with the side chains of Asn185, Gln218, and Gln236 (Figure 3a). In addition, N1 of the adenine ring approaches within hydrogen bonding distance of the peptide bond amide nitrogen and carbonyl oxygen of Asp214. These interactions provide a basis for the unique requirement for MgATP in nitrogenase catalysis and are largely conserved in the structure of the Fe protein within the nitrogenase complex stabilized with MgADP and tetrafluoroaluminate (Figure 3b). One notable exception is the side chain of Arg213 that in the complex structure was found to be in proximity to the nucleotide such that the guanidinium ring of the side chain is stacking with the adenine ring. In contrast, in the MgADP-bound Fe protein structure presented here, the Arg213 side chain is well-ordered in electron density maps and found to be located a farther distance from the nucleotide (not shown), potentially a result of the absence of the dramatic rigid-body reorientation of the Fe protein monomers observed in the complex. In the Fe protein of the complex, the position of the side chain of Arg213 is stabilized by an intersubunit salt bridge involving Glu154. This interaction is not observed in the MgADP-bound Fe protein structure, and the side chains of Arg213 and Glu154 are located ~10 Å from one another. The ribose moiety is hydrogen bonded to the protein through the side chain oxygen of Glu221. The phosphate-binding loop region (P-loop) of the Fe protein, which is a common Gly-X-X-Gly-X-Gly motif (where X represents no consensus at this position) (*23*) found in other nucleotide binding proteins, is found to contribute to all the direct interactions of the protein with the phosphates through hydrogen bond interactions provided by residues 10−17. These interactions are conserved to a large extent in the nitrogenase complex stabilized by MgADP and tetrafluoroaluminate (*11*); however, the cross-subunit interactions observed in the complex involving Lys15 and Asp129 are also not observed in the structure of the Fe protein with MgADP bound. In addition, there are some changes resulting from the addition of tetrafluoroaluminate that will be discussed below. Interestingly, when the P-loop region of the MgGDP off state of ras P21 (*5*) is superimposed on an Fe protein monomer using the Cα atoms of the individual phosphate-binding loop regions, the position and orientation of MgADP and MgGDP in the two structures are strikingly similar (Figure 3c). This illustrates that the

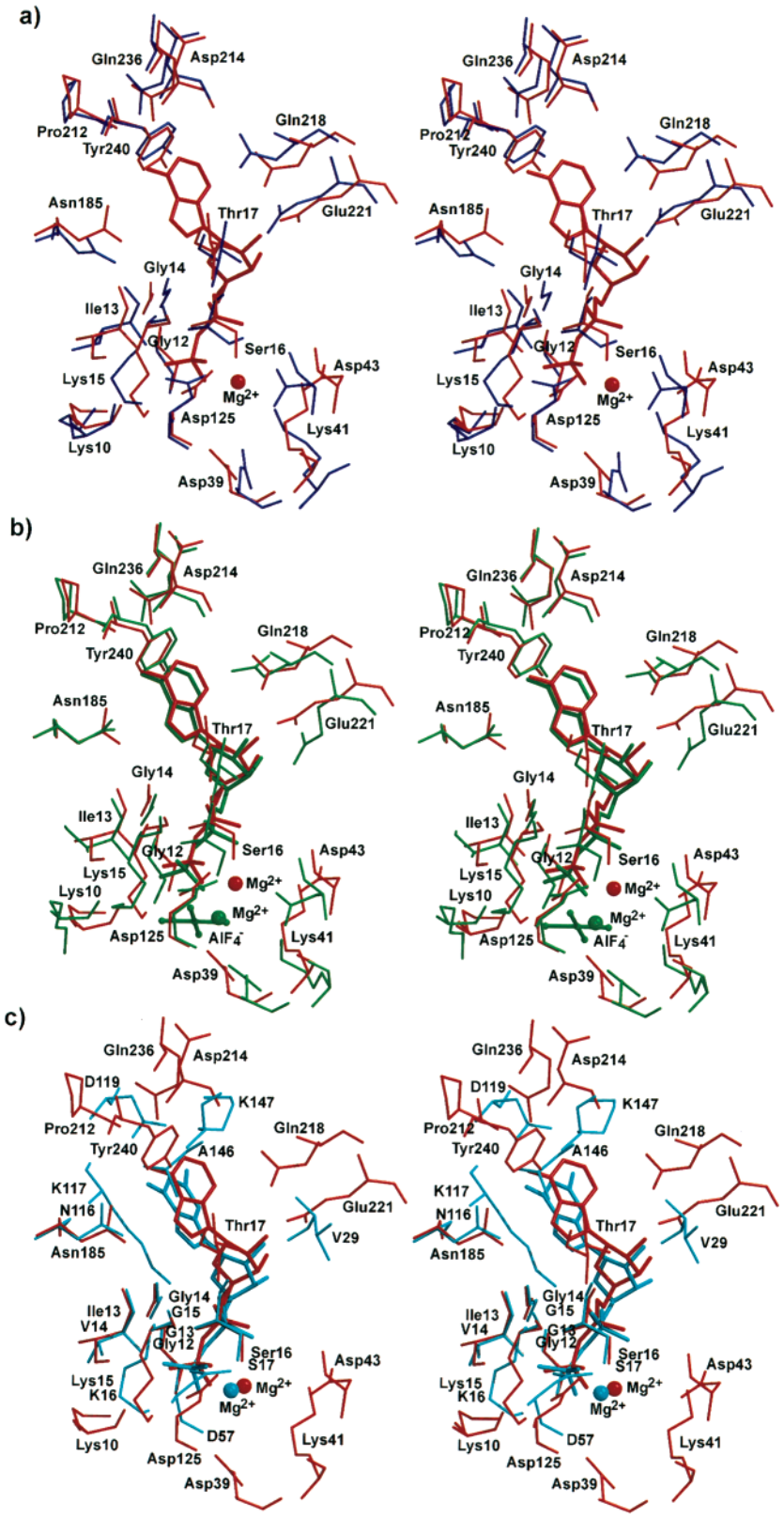

FIGURE 3: Nucleotide binding region. (a) Wall-eyed stereoview of the superposition of the nucleotide binding region of the Fe protein in the presence of MgADP (red) and nucleotide free Fe protein [2nip (blue)], (b) the Fe protein in the presence of MgADP AlF_4^- [1n2c (green)] in the Fe protein−MoFe protein stable complex. All corresponding Cα atoms of a single Fe protein monomer from 2nip and 1n2c were used for superposition onto the MgADP-bound Fe protein structure described herein, and (c) the superposition of the nucleotide-binding region of the Fe protein with MgADP bound (red) and for ras P21 with MgGDP bound (cyan). The superposition was generated by the alignment of corresponding Cα atoms with the phosphate binding loops of MgGDP-bound ras P21 and the MgADP-bound nitrogenase Fe protein.

interaction between the P-loop and the bound Mg^{2+} ion and phosphates of ADP is similar for these two proteins and is key in defining the conformational states relevant to the protein's respective functions.

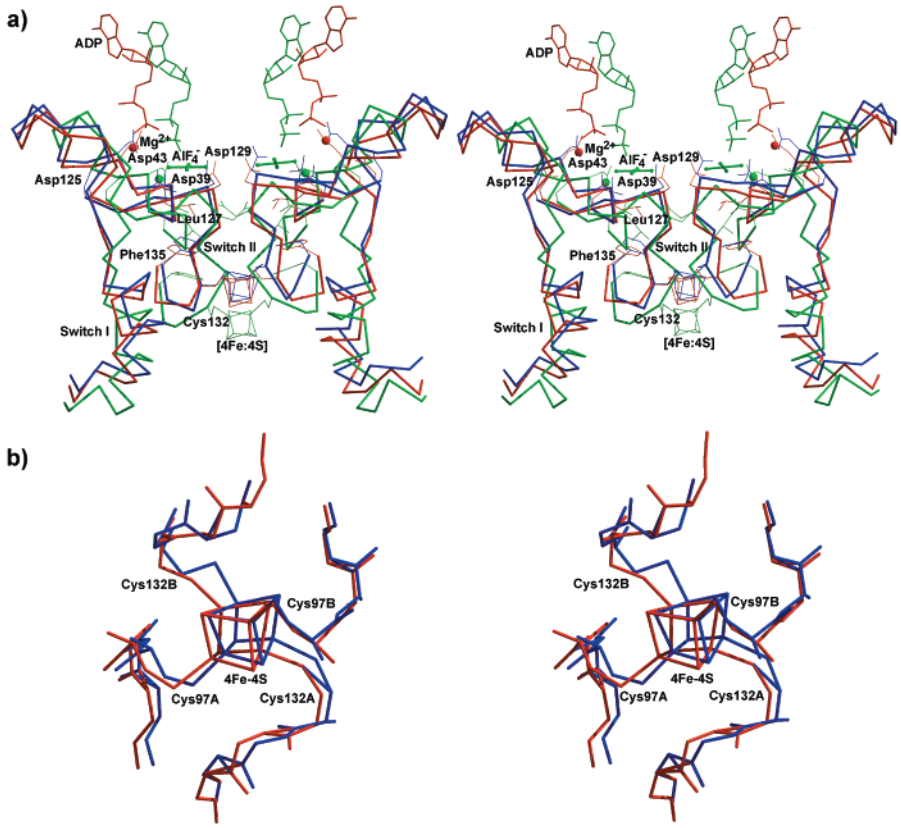

FIGURE 4: Nucleotide switches and the [4Fe-4S] cluster. (a) Wall-eyed stereoview of the superposition of switches I and II and the [4Fe-4S] cluster for the Fe protein structures with no nucleotides bound (blue), with MgADP AlF_4^- bound with the complex (green), and with MgADP bound (red). The side chains of several amino acid residues are shown, along with MgADP (red) and MgADP AlF_4^- (green) and (b) the [4Fe-4S] cluster coordination environment, including the coordinating ligands and adjacent residues, are shown for the nucleotide free Fe protein (blue) and the MgADP-bound Fe protein (red).

Two of the more intriguing unanswered questions with respect to the Fe protein's involvement in nitrogenase catalysis are (i) how the binding and hydrolysis of nucleotides are linked to protein conformational changes that result in specific alterations in the properties of the [4Fe-4S] cluster and (ii) how the binding of nucleotides controls the association of the Fe protein with the MoFe protein. A better understanding of these issues will contribute to our overall understanding of how intermolecular electron transfer is related to MgATP hydrolysis. The current structure of the Fe protein with MgADP bound provides insights into both of these questions. Two regions within the Fe protein are observed to undergo significant structural changes depending on the nucleotide-bound state of the Fe protein (Figure 4). One region is defined by Asp125, which interacts with the bound Mg^{2+}, through Cys132, which provides two of four ligands to the [4Fe-4S] cluster. This region of the Fe protein has been termed switch II by analogy to a homologous region found in ras P21 (*24*, *25*). A second region of the Fe protein observed to undergo nucleotide-dependent structural changes goes from Asp39, which interacts with the bound Mg^{2+}, to amino acids in the region of residues 59−69, which interact with the MoFe protein. This region of the Fe protein has been termed switch I by homology to a similar switch observed in ras P21 (*26*).

Switch II provides a mechanism for communication between the nucleotide-binding site and the [4Fe-4S] cluster (*25*, *27*). Superposition of the nucleotide free Fe protein structure upon that of the MgADP Fe protein in the environment of the [4Fe-4S] cluster shows that the Cys132 ligands of the cluster experience a change in conformation while the Cys97 ligands remain largely unchanged (Figure 4b). Binding of MgADP exerts small changes on the conformation of the P-loop regions that are in turn communicated to the cluster through a hydrogen bonding interaction of the main chain amide of Gly14 to the side chain of Asp129. Interestingly, substitution of Asp129 with Glu results in an Fe protein that in its nucleotide free state has biophysical properties similar to those of the native Fe protein with bound nucleotides (*28*). This is in contrast to the Fe protein in the nitrogenase complex stabilized with MgADP and tetrafluoroaluminate in which all four ligands of the [4Fe-4S] cluster adopt different conformations (*11*). The individual contributions of nucleotide binding and complex formation to the changes in the environment of the [4Fe-4S] cluster represent an elegant mechanism by which the biophysical properties of the cluster can be regulated during enzyme catalysis.

Switch I provides a mechanism for communication from the nucleotide-binding site to the Fe protein surface involved in interactions with the MoFe proteins. It appears that the hydrolysis of MgATP to MgADP decreases the affinity of the Fe protein for the MoFe protein following electron transfer, thus allowing the two proteins to dissociate (*26*, *29*, *30*). Switch I provides a mechanism for propagation of the change from the MgATP-bound state to the MgADP state to the surface of the Fe protein to control protein−protein interaction.

A closer look at the interactions between the Fe protein and the Mg^{2+} and phosphate portions of the bound MgADP

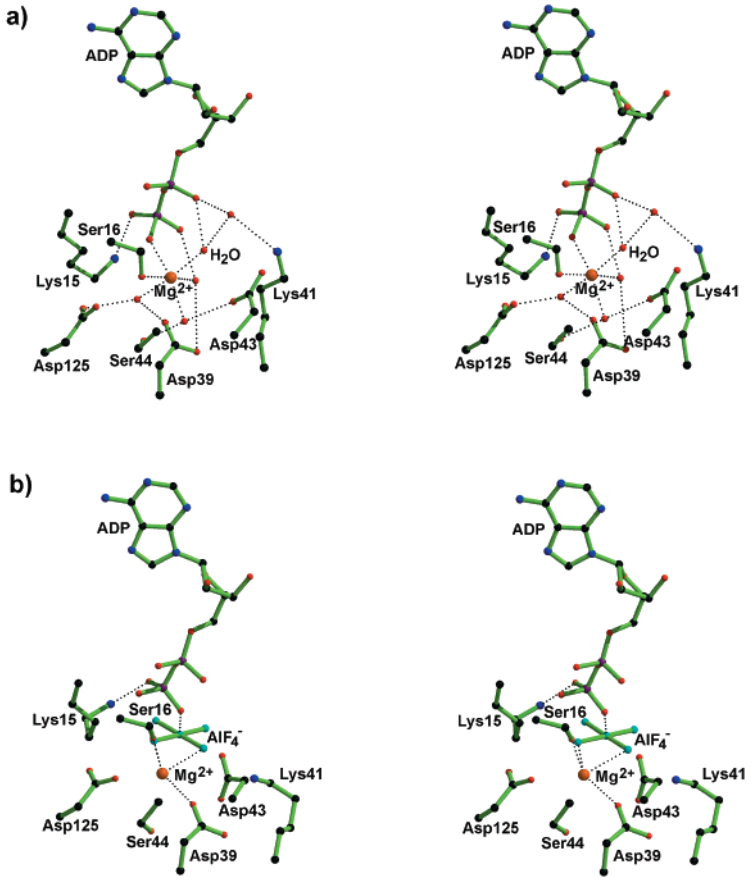

FIGURE 5: Protein interactions with the phosphate region. (a) Wall-eyed stereoview of the region of the Fe protein within a single subunit coordinating the phosphates of the ADP and the Mg^{2+} ion coordination in the MgADP-bound Fe protein and (b) the Fe protein with the nitrogenase complex stabilized by MgADP AlF_4^-.

reveals likely mechanisms for communication of the ATP hydrolytic event to changes in switches I and II (Figure 5). It was proposed previously that the change of the Mg^{2+} from interaction with the β- and γ-phosphates to the α- and β-phosphates was a driving step for nucleotide hydrolysis (*14*, *31*). Analysis of the structures of the Fe protein with MgADP and MgADP AlF_4^- bound (*11*) supports the model which holds that protein interactions with the Mg^{2+} are essential to the transduction of the nucleotide hydrolysis event. In the structure of the Fe protein with MgADP bound, the octahedral coordination environment of the Mg^{2+} consists of four bound water molecules, the side chain O atom of Ser16, and an O atom of the β-phosphate. The water molecules bound by the Mg^{2+} ion interact with switch I through hydrogen bonding with the side chain oxygen atoms of Asp39, Asp43, and Ser44 (Figure 5). The Mg^{2+} ion in the Fe protein of the complex is clearly different with two F atoms of the tetrafluoroaluminate serving as direct ligands, leading to repositioning of the residues of swtich I. It is apparent that differences in the coordination of the Mg^{2+} ion transduce the different signals to the docking interface through direct interactions with residues of switch I.

The structure of the MgADP state presented here provides an opportunity to differentiate the individual contributions arising from nucleotide binding, nitrogenase complex formation, and complex-dependent nucleotide hydrolysis in the catalytic mechanism of this complex enzyme.

ACKNOWLEDGMENT

The efforts of Mi Suk Jeong in the preparation of this paper are gratefully acknowledged. The SSRL Biotechnology Program is supported by the National Institutes of Health, National Center for Research Resources, Biomedical Technology Program, and by the Department of Energy, Office of Biological and Environmental Research.

REFERENCES

1. Koonin, E. V. (1993) *J. Mol. Biol. 229*, 1165−1174.
2. Schultz, G. E. (1992) *Curr. Opin. Struct. Biol. 2*, 61−67.
3. Story, R. M., and Steitz, T. A. (1992) *Nature 355*, 374.
4. Kjeldgaard, M., and Nyborg, J. (1992) *J. Mol. Biol. 223*, 721−742.
5. Tong, L., DeVos, A. M., Milburn, M. V., and Kim, S. H. (1991) *J. Mol. Biol. 217*, 503−516.
6. Schlessman, J. L., Woo, D., Joshua-Tor, L., Howard, J. B., and Rees, D. C. (1998) *J. Mol. Biol. 280*, 669−685.
7. Howard, J. B., and Rees, D. C. (1996) *Chem. Rev. 96*, 2965−2982.
8. Georgiadis, M. M., Komiya, H., Chakrabarti, P., Woo, D., Kornuc, J. J., and Rees, D. C. (1992) *Science 257*, 1653−1659.
9. Shah, V. K., and Brill, W. J. (1977) *Proc. Natl. Acad. Sci. U.S.A. 74*, 3249−3253.
10. Hageman, R. V., and Burris, R. H. (1978) *Proc. Natl. Acad. Sci. U.S.A. 75*, 2699−2702.
11. Schindelin, H., Kisker, C., Schlessman, J. L., Howard, J. B., and Rees, D. C. (1997) *Nature 387*, 370−376.

12. Seefeldt, L. C., Morgan, T. V., Dean, D. R., and Mortenson, L. E. (1992) *J. Biol. Chem. 267*, 6680−6688.
13. Leslie, A. G. W. (1992) *Joint CCP4 and ESF-EACBM Newsletter on Protein Crystallography*, Vol. 26, Daresbury Laboratory, Warrington, U.K.
14. Seefeldt, L. C., and Mortenson, L. E. (1993) *Protein Sci. 2*, 93−102.
15. Navaza, J. (1994) *Acta Crytallogr. A50*, 157−163.
16. Jones, T. A., Zhou, J. Y., Cowan, S. W., and Kjeldgaard, M. (1991) *Acta Crystallogr. A47*, 110−119.
17. Brunger, A. T. (1992) *Nature 355*, 472−474.
18. Brunger, A. T., Kuriyan, J., and Karplus, M. (1987) *Science 235*, 458−460.
19. Laskowski, R. A., McArthur, M. W., Moss, D. S., and Thornton, J. M. (1993) *J. Appl. Crystallogr. 26*, 283−291.
20. Esnouf, R. M. (1997) *J. Mol. Graphics 15*, 132−134.
21. Merritt, E. A., and Murphy, M. E. P. (1994) *Acta Crystallogr. D50*, 869−873.
22. Nichols, A., Sharp, K. A., and Honig, B. (1991) *Proteins 11*, 281−296.
23. Walker, J. E., Saraste, M., Runswick, M. J., and Gay, N. J. (1982) *EMBO J. 1*, 945−951.
24. Howard, J. B., and Rees, D. C. (1994) *Annu. Rev. Biochem. 63*, 235−264.
25. Ryle, M. J., and Seefeldt, L. C. (1996) *Biochemistry 35*, 4766−4775.
26. Lanzilotta, W. N., Fisher, K., and Seefeldt, L. C. (1997) *J. Biol. Chem. 272*, 4157−4165.
27. Wolle, D., Dean, D. R., and Howard, J. B. (1992) *Science 258*, 992−995.
28. Lanzilotta, W. N., Ryle, M. J., and Seefeldt, L. C. (1995) *Biochemistry 34*, 10713−10723.
29. Duyvis, M. G., Wassink, H., and Haaker, H. (1996) *FEBS Lett. 380*, 233−236.
30. Renner, K. A., and Howard, J. B. (1996) *Biochemistry 35*, 5353−5358.
31. Lowe, D. J., Ashby, G. A., Brune, M., Knights, H., Webb, M. R., and Thorneley, R. N. F. (1995) in *Nitrogen Fixation: Fundamentals and Applications* (Tikhonovich, I. A., Provorov, N. A., Romanov, V. I., and Newton, W. E., Eds.) pp 103−108, Kluwer Academic, Dordrecht, The Netherlands.

BI001705G